NUMERICAL CALIBRATION OF MECHANICAL BEHAVIOUR OF COMPOSITE SHELL TUNNEL LININGS

Authors:

- Jiang Su[1] sujiang.uk@gmail.com
- Alan Bloodworth[2] a.bloodworth@warwick.ac.uk

Affiliations:

(1) Tunnels, AECOM, Croydon, UK

(2) School of Engineering, University of Warwick, UK

Highlights:

- Four-point bending tests were carried out on composite shell lining beam samples
- Strain distribution across composite lining cross-section identified
- Numerical analyses verified the suggested range of interface stiffnesses
- Proposed numerical model was capable of predicting the composite mechanical behavior
- Sensitivity study investigates the impact of interface stiffnesses and position

Abbreviations

SCL: Sprayed concrete lined

CSL: Composite shell lining

DCA: Degree of Composite Action

DSL: Double shell lining

EVA: Ethylene Vinyl Acetate

FE: Finite Element

FD: Finite Difference

Abstract:

Composite shell linings consist of primary and secondary sprayed concrete linings separated by a layer of spray-applied waterproofing membrane. In order to design such a lining configuration, a calibrated numerical simulation approach is needed and the impact of interface properties on the composite mechanical behaviour should be understood.

A programme of laboratory tests was carried out on beam samples cut from composite shell test panels and subjected to four-point bending under short-term loading. A range of membrane thicknesses and substrate roughness were compared and composite mechanical behaviour quantification methods developed. The behaviour of composite beams was understood and the strain distribution across composite lining cross-section was identified.

A numerical model by the finite difference method was then set up for the beams and verified against the test data. With interface stiffnesses obtained from previous element tests, the composite beam model is capable of predicting the strain distribution across the cross-section and real behaviour of composite beam members to within an acceptable level of accuracy taking into account variations arising from workmanship. Sensitivity studies were carried out to understand the impact of interface properties and membrane interface position on the degree of composite action.

Key words:

Spray-applied waterproofing membrane

Composite mechanical behaviour

Introduction

Sprayed concrete lined (SCL) tunnel has seen rapid development over the last twenty years in the UK (Su, 2013). Three of these developments have been the inclusion of wet-mix sprayed concrete primary lining as part of the permanent load-bearing structure, the replacement of the traditional sheet membrane between the primary and secondary linings with a double bonded spray-applied waterproofing membrane and use of a wet-mix sprayed or cast in-situ concrete secondary lining. This innovative configuration is called a *composite shell lining* (CSL) and has recently been adopted in projects in the UK and other European countries (Pickett, 2013; Holter et al., 2013; Hasik et al 2015) in soft ground of low permeability.

While the design of traditional SCL tunnels, consisting of sacrificial sprayed concrete primary lining, sheet waterproofing membrane and permanent cast in-situ concrete secondary lining, has become relatively mature and is backed with many successful case histories, the design of CSL is still at its infant stage. In most cases the CSL tunnels are designed as the *double shell lining* (DSL) tunnels, which is a similar lining configuration to CSL but assuming an unbonded (i.e. no tension nor shear but only compressive stiffness assumed) waterproofing interface sandwiched between the two layers of linings (Pickett, 2013). It has been claimed that, if composite action is considered in the design, the CSL could achieve 20%-30% overall lining thickness reduction when compared with traditional SCL tunnels under the same ground conditions (Pickett and Thomas 2011).

In order to achieve an efficient design for CSL tunnels, two issues need to be resolved: (1) understanding of the mechanical properties of the spray-applied membrane interface under realistic humidity conditions, and (2) a calibrated modelling methodology for simulating the composite mechanical behaviour of composite shell linings.

Research on the membrane interface material has been gradually providing understanding of its function and mechanical properties (Verani and Aldrian, 2010; Thomas, 2010; Nakashima et al., 2015; Su and Bloodworth, 2016; Holter and Geving, 2015; Holter, 2016), and its main findings will be discussed in the following section. This paper focuses on the second issue on modelling methodology. Once the modelling methodology is validated, it can then be applied to a full CSL tunnel, with considerations of factors that are essential to CSL tunnel design such as soil-structure interaction,

stage construction, *etc*. By doing so, it is expected that the general behaviour of CSL tunnels may be understood, a set of design principles derived and the CSL tunnel proved to be an efficient lining form. In this paper, a set of laboratory flexural tests on CSL beams is presented and a numerical analysis methodology for simulating the composite mechanical behaviour of CSL is developed and calibrated against the flexural test results. A sensitivity study on the spray-applied membrane interface properties is undertaken to evaluate the impact of varying interface stiffness (caused by for example different types of membrane, impact of different temperature or humidity conditions, or long-term creep effects) and membrane interface position on the composite mechanical behaviour of CSL beams. A unified parameter, 'degree of composite action' (*DCA*), is developed to quantify the composite mechanical behaviour of laboratory tested and numerically modelled CSL beams.

Technical background

For tunnelling waterproofing purposes, there are currently two types of spray-applied membrane: Ethylene-Vinyl-Acetate copolymer (EVA) based products and methyl methacrylate resin based products. The membranes discussed in this section, used in the following described laboratory composite beam tests and to calibrate the numerical model, are all EVA-based products.

Until now there has been limited literature published on the laboratory testing or numerical analysis of composite mechanical behaviour for CSL tunnels.

Verani and Aldrian (2010) reported three-point bending tests on a pure sprayed concrete and a composite beam with spray-applied waterproofing membrane sandwiched half-depth under ambient laboratory climate conditions (e.g. 15-20° in temperature and 40-60% relative humidity), showing the composite beam had 50% of the peak flexural strength of the pure sprayed concrete beam, but greater residual flexural strength. Thomas (2010) analysed a CSL tunnel to obtain load-sharing ratios between the linings with interface shear stiffness varied between a full-slip (non-composite action) to a non-slip (fully-composite action) case, and pointed out that the CSL tunnel lining should be partially composite if realistic membrane interface stiffnesses are used. Nakashima *et al*. (2015) presented flexural test results on two CSL beams with and without axial force again under ambient laboratory climate conditions. For a beam tested without axial force, although the strains and midspan deflections did not

match theoretical values for a fully-composite beam, the authors nevertheless concluded that the CSL beams were fully composite and that there was a problem with the strain measurement. In fact, the CSL beams were only partially composite and would be expected to have larger deflections and different strain distributions compared to sprayed concrete beams under the same loading.

Su and Bloodworth (2016) carried out a comprehensive laboratory testing programme on element specimens cut from CSL sprayed panels with different primary lining substrate surface preparations and membrane thicknesses, loaded in compression, tension and shear under ambient laboratory climate conditions. The impacts of substrate surface preparation and membrane thickness on the interface parameters were investigated.

All the above reported laboratory tests were carried out on samples that were essentially 'dry', i.e. were being tested under ambient laboratory conditions without the samples being in contact with or immersed in water such as might be the case if a crack in a primary lining in water-bearing ground led to water contacting the extrados of the membrane. Field measurements by Holter and Geving (2015) on a rock SCL tunnel with spray-applied waterproofing found the moisture content of the membrane to vary between 30% and 40%, determined by the moisture properties of the concrete and the membrane, as well as the interfaces between the two materials. Further research by Holter (2016) suggested that high moisture content in the EVA-based polymer membrane may affect its mechanical properties, e.g. reduce its tensile strength. More research is needed on this topic, particularly to quantify the membrane moisture content in soft ground applications of CSL and then to go on to obtain the membrane mechanical properties under those conditions. In the meantime, the main purpose of this paper is to provide a calibrated numerical modelling methodology for simulating the composite mechanical behaviour of CSL tunnels. The calibration of the model is from laboratory tests in ambient conditions, which is understood do not relate to completely realistic in-situ conditions. However, once the calibration of the model is done, the model is used in a parametric study to investigate the effect on the behaviour of composite beams of varying of interface parameters such as membrane stiffness that are known from the research carried out by Holter (2016) to be a function of membrane saturation.

Composite mechanical behaviour

CSL beams consist of two layers of component beams, representing the primary and secondary linings, and a sandwiched layer of membrane interface. The stress and strain distributions through the cross-section will depend on the degree of composite action, as shown in Figure 1. As this reduces from fully-composite to non-composite, neutral axes for each component beam move away from the membrane until they reach half-depth of each component. Applying Euler-Bernoulli beam theory with an assumption of linear elastic behaviour, the lower the degree of composite action, the lower the moment (calculated from the stress blocks) for a given deformation (curvature), and hence the lower the flexural stiffness of the lining.

The *DCA* may be quantified based on beam deflection as follows (Frankl *et al.* 2011):

$$DCA = \frac{k_{comp} - k_{non}}{k_{full} - k_{non}} \qquad (1)$$

Where k_{comp}, k_{non} and k_{full} are equivalent flexural stiffness of the composite, non-composite and fully-composite beam respectively under any given loading and support condition. Equivalent flexural stiffness is calculated from the slope of the load-deflection lines between two loading levels in the tests. The range of DCA is between 0.0 (non-composite) and 1.0 (fully-composite). An alternative definition of *DCA* is based on longitudinal strains of composite and fully-composite beams:

$$DCA = \frac{\varepsilon_{1/2comp}}{\varepsilon_{1/2full}} \qquad (2)$$

Where $\varepsilon_{1/2comp}$ and $\varepsilon_{1/2full}$ are longitudinal strains of the composite and fully-composite beam respectively at the half depth of either top or bottom component beam, as annotated in Figure 1. $\varepsilon_{1/2full}$ can sometimes be substituted by halving the strain $\varepsilon_{surf-full}$ either top or bottom of a fully-composite beam.

The third definition of *DCA* is based on the relative component beam end displacements of composite and fully-composite beams:

$$DCA = \frac{d_{1/2comp}}{d_{1/2full}} \qquad (3)$$

Where $d_{1/2comp}$ and $d_{1/2full}$ are relative displacement between the top and bottom component beams at their respective half-depths.

In this research, all laboratory tested and numerically predicted results are expressed in the form of degree of composite action, to quantify the composite mechanical behaviour and to ease the comparison.

Research methodology

Layout of the work

This paper presents the calibration of a numerical modelling methodology for simulating composite mechanical behaviour against laboratory flexural test results on CSL beams, followed by a numerical sensitivity study on the impact of membrane interface properties and positions. The content is presented in three parts as described below.

The first part reports testing on flexural tests on beam samples cut from the same steel fibre-reinforced test panels as previous research (Su and Bloodworth, 2016), to explore the degree of composite action present in the lining in flexure under ambient laboratory climate conditions.

The second part presents numerical simulations of the beams to verify the applicability in the beam tests of the range of interface stiffnesses suggested by the previous element tests (Su and Bloodworth, 2016). Sensitivity analyses have also been performed to explore the effect of interface parameters such as interface stiffness and interface position on the expected composite mechanical behaviour.

The third part is a discussion of results. This includes the relationship of the laboratory specimens to the conditions in a typical tunnel, effect of small scale and short-loading loading, interpretation and discussion of measured values, numerical simulation predictions and finally a synthesis of findings.

Evaluation of the degree of composite mechanical behaviour from laboratory test values

Historically, most fibre-reinforced SCL was used in rock tunnels, where lining performance criteria in most standards focus on the post-peak strength, large deformation stage (NCA, 2011; CIA, 2011; RILEM, 2003; fib, 2013). In soft ground SCL tunnels, the lining is normally designed to function in its pre-peak stage, and it is therefore more pertinent to examine the degree of composite action in this pre-peak stage.

The degree of composite action is evaluated from pre-peak load-deflection, longitudinal strain and beam end relative displacement laboratory data. A brief assessment of the composite action in the post-peak region of behaviour was also carried out.

Modelling strategy

Finite difference software FLAC (Itasca, 2008) was used for simulating the behaviour of the pure sprayed concrete and composite beams. This software adopts an explicit analysis approach, in which iteration is used to advance a solution through a sequence of steps from a start to a final converged state. This approach is very efficient in simulating both the interface mechanical behaviour (Bergado and Teerawattanasuk, 2008; Green and Ebeling, 2003; Chen and Martin, 2002) and the nonlinear soil-structure interaction (Thomas, 2003, Jones, 2007, Jones et al., 2008), both of which are essential for the next stage of research.

Traditionally, beam elements are used for representation of primary and secondary linings within an SCL tunnel in 2D plane strain finite element or finite difference analysis. While providing a certain degree of convenience in building SCL linings, this approach cannot simulate the composite mechanical behaviour between the two layers of linings, mainly due to the implicit thickness property of the beam elements. In FLAC, materials can be represented either by elements as described above, or by zones, which form a grid with physical thickness. Zones can be assigned either with linear or nonlinear stress-strain constitutive laws, to simulate the behaviour of particular materials. For this research, zones are used for the primary and secondary linings.

Interface elements are a special feature of FLAC, the properties of which may be characterised by Coulomb sliding and/or tensile separation (Itasca, 2008). They can be used to represented a normal and a shear stiffness between two planes which may or may not contact to each other. For this research, interface elements are used for the sprayed membrane interface.

The explicit thickness property of the zones and the ability of the interface elements to transfer adhesive and shear stresses between two layers of zones enable composite action between the primary and secondary linings to be simulated correctly.

Sensitivity study for variance in practice

SCL is a technique the quality of which is heavily affected by the workmanship. Although laser scan total stations and automatic spraying robots have been introduced in recent SCL projects (Batty et al., 2016) variances of the lining geometry, thickness and substrate roughness from the design is

unavoidable, and these variances are usually considered as tolerances but not explicitly numerically simulated. In addition, different types of spray-applied membrane under varying external conditions (e.g. temperature and humidity) may have different interface properties. Therefore, a sensitivity study was carried out to investigate the impact of varying interface properties to encompass these variances on the mechanical behaviour of the SCL beams.

Four-point bending tests

The standard test configuration for determining the flexural strength and stiffness properties of fibre-reinforced sprayed concrete is either three- or four-point bending on a beam sample sprayed in a mould or cut from a larger sprayed panel (BSI, 2006; BSI, 2005a). Four-point (without notch) bending tests [23] were used in this study. These are preferred over three-point notched bending tests [24] as they avoid unfavourable stress concentration at the notch and provide a region of constant moment to facilitate strain measurement and comparison with a model. Configuration of the test and nominal dimensions of the composite beam specimens are shown in Figure 2. A longer constant bending zone of 400 mm was used compared to the standard length of one-third of the overall beam length in order to minimise the significance of shear deformation and generate purer flexural behaviour (ACI, 2008). Linear potentiometers and strain gauges were used to record midspan vertical displacement, longitudinal relative beam end displacement and longitudinal strains for evaluation of the degree of composite action and for model verification. *P* is the total loading on the beam.

Three sprayed concrete beams (without sandwiched membrane) were also tested and the results used to back-calculate the Young's modulus of concrete (*E*) (assumed isotropic) from the deflection and longitudinal strain data using the following equations:

$$\omega_{max} = 11PL^4/396EI \qquad (4)$$

$$\varepsilon_{1/2} = 3PL/8Ebh^2 \qquad (5)$$

Where *L* is the span between two supports, *I* the second moment of area of the beam cross-section, *b* and *h* the width and height of the cross-section of the beam, ω_{max} the vertical displacement at midspan and $\varepsilon_{1/2}$ the strain at half depth (either top or bottom component).

Specimens

Sprayed concrete wet mix specification and design are given in Tables 1 and 2 respectively. A commercially-available EVA-based waterproofing membrane was used. This product contains more than 75% by weight of EVA co-polymer, and its functional properties are expected to be similar to other EVA-based membranes. The spray was carried out at the contractor's plant facility and the direction of all spray was perpendicular to the test box (BSI, 2005b). After each spray, the boxes were covered with plastic sheeting, simulating a realistic environment for the underground. The spray was carried out during the summer (June –August 2011) in the UK, with daily temperatures ranging from 15-25 degrees Celsius.

Table 1 Mix specification for primary and secondary lining sprayed concrete

Mix	Description	Agg Size (mm)	Cement Type	Targeted Slump	Targeted 90-day Strength
20080778	P450 HP-PLA sprayed concrete mix	8	CEM1	S3	40MPa

Table 2 Mix design for primary and secondary lining sprayed concrete

Materials*	DRY Batch Weights kg/m^3
Type	20080778
CEM1	450
0/4 MP Sand	1300
4/10 Gravel	550
Water reducing admixture	2250
Steel fibre	40
Accelerator	6% (weight of cement)
Superplasticiser	0.9% (weight of cement)
Target W/C	0.45

*Further details of materials used are given in Appendix A

Samples were prepared with three alternative surface types for the primary lining substrate – as-sprayed (rough), smoothed (float finish flat surface) and regulated (smoothed by application of a regulating layer of gunite of smaller aggregate size without steel fibres (ITA, 2013)). The sprayed

concrete and sprayed membrane interface properties (e.g. strength and stiffness) can be found in Su & Bloodworth (2016).

Seven composite beams, with various combinations of substrate roughness and membrane thickness, were tested as well as three pure sprayed concrete beams (Table 3). Details of the procurement of the beam test samples are described in Su & Bloodworth (2016). After transport to the University, the beams were kept inside the laboratory under conditions of ambient temperature and humidity and ready for tests

Beams were tested in two groups, A and B, approximately 6 months and 54 months respectively after spray. Maximum ratio of membrane thickness to overall beam depth is 6.7% (10 mm/150 mm for beam A5-11), and maximum deviation of membrane position from half-depth is 9.3% (7 mm/75 mm for beam B4-12). Both are less than 10%, within the acceptable level of construction tolerance. The thickness of the membrane and primary and secondary lining was the average value from 10 measurements at characteristic points.

Table 3 Dimensions of test beams

Test group	Beam Ref.	Measured membrane thickness (mm)	Substrate preparation	Thickness of secondary lining: Top component beam (mm)	Thickness of primary lining: Bottom component beam (mm)
A	A1-11	4	smoothed	77	69
	A2-11	3	regulated	70	77
	A3-11	3	as-sprayed	67	80
	A4-11	6	smoothed	69	5
	A5-11	10	regulated	70	70
	A7-11	N/A	N/A	150 total depth, sprayed concrete	
B	B4-12	6	smoothed	65	79
	B4-13	5	smoothed	65	80
	B7-12	N/A	N/A	150 total depth, sprayed concrete	
	B7-13				

Test setup and experimental procedure

Test setup for Group A is shown in Figure 3 (a). Machine loading was applied through a yellow steel crossbeam equally to two roller bearings, each on a spreader plate to distribute the loads more uniformly to the beam, as shown in Figure 3 (b). One linear potentiometer measured vertical downward displacement of the top of the beam at midspan. Four strain gauges were attached to measure longitudinal strain, at half depth of the top and bottom component beams on each side at midspan (Figures 2 and 3 (c)). Two potentiometers located at one end of the beam recorded longitudinal relative beam end displacements (Figure 3 (d)).

In Group B the overall setup was the same but there were differences in the instrumentation. Two potentiometers were positioned at midspan, one each side of the beam top surface, to detect any component of beam torsion. The four longitudinal strain gauges were arranged to obtain more precise strain profiles through the beams, with two at half-depth of the top component beam (one each side of the beam) and the third and fourth on the top and bottom surfaces of the beam on its centreline (Figure 2).

For all beams, machine stroke control was used with a loading rate of 0.01 mm/s to a vertical displacement of approximately 10 mm.

A steel I-section beam of similar dimensions to the concrete beams and with second moment of area of 8.2×10^6 mm^4 was tested under the same configuration and loading procedure to determine the test setup compliance, which was approximately 0.0142 mm/kN. This was used to correct the test results for the SCL beams.

Variance in samples arising from workmanship

The laboratory four-point bending test results and their derived degree of composite action are inevitably affected to some extent by the limitations in workmanship of the test specimens. Three variances in sample geometry compared to an idealised composite beam with interface of negligible thickness at half-depth have been identified:

(1) Variance in cross-section, with slight difference in section depth between the two sides.

(2) Variance in interface position, with it deviating from half overall depth of the beam.

(3) Variance in finite thickness of membrane interface.

These variances complicate the process of obtaining the degree of composite action using equations (1) and (2) and are difficult to incorporate in numerical models. Nevertheless, it is important to identify and assess the impact of these variances, which will be evaluated and discussed in following sections.

Validation of sprayed concrete stiffness

For Group A beams, Young's modulus of 20 GPa was assumed, obtained from compression tests on three sprayed concrete cylinder samples tested at the same time as the beams [13]. For Group B beams, which experienced further curing before testing, a Young's modulus of 22 GPa was obtained by back-analysis of the load-deflection and longitudinal strain data for sprayed concrete beams B7-12 and B7-13 using equations (4) and (5), as illustrated in Figures 4 and 5 respectively.

Crack propagation

All beams exhibited similar crack development. This is shown in Figure 6 for beam A2-11 and detailed as follows for that beam.

1. A visible crack was first observed when the load reached 19 kN (90% of peak load).
2. A single flexural crack was observed in all tests.
3. The crack was developing and approaching the membrane when the peak load was reached.
4. With the crack having crossed the membrane and extended to ¾ of overall beam depth, the beam could still sustain 18.5 kN (88% of peak load), At crack length 80% of beam depth it could sustain 10 kN (50% of peak load).
5. Steel fibres were observed to fail in the desired pull-out mode (providing confidence in ductile behaviour) rather than by rupture.

Comparing the load-deflection graph and observations of cracking, it is evident that the beams entered nonlinear behaviour before visible cracks were observed, implying invisible cracking much earlier than visible cracks (Bloodworth and Zhou, 2014).

Flexural response

Load-deflection diagrams for Group A and B beams are shown in Figures 7 and 8 respectively. A typical pattern is seen of linear behaviour up to peak load, followed by a sudden load drop and then steady load decrease. The only major exception is beam B4-12, which has a lower and much less pronounced peak load, possibly due to unnoticed prior micro-cracking.

Pre-peak load-deflection relationships for all beams are shown in Figure 9, together with theoretical upper and lower limits representing fully-composite and non-composite beams assuming 20 GPa Young's modulus. Group A beams A2-11 and A7-11 appear unexpectedly stiff, and A5-11 was unexpectedly soft (above 10 kN load), possibly an artefact of the use of only one linear potentiometer for Group A which was unable to detect torsion of the beam under load (Type (1) variance). In this case, the top surface of the beam may rotate towards one side when under loading, resulting in excessive beam deflection on that side. The Group B beams, for which deflection was evaluated as the average from two potentiometers, show improved accuracy for the deflection reading and lie consistently between the limits, strongly suggesting that a certain degree of composite mechanical behaviour exists across the interface. The initial softer behaviour of beam B4-12 is due to a "bedding" effect.

Pre-peak degree of composite action from laboratory load-deflection relationships

Pre-peak load performance of composite and sprayed concrete beams is compared in Table 4. Equivalent flexural stiffness for composite beams is calculated from the linear portion of the graph not affected by the "bedding" effect during the initial loading or the "softening" effect near the peak stresses. The range of composite action is calculated based on equation (1), using test data from the two sprayed concrete beams B7-12 and B7-13 to obtain k_{full}. k_{non} is taken as a quarter of k_{full}, because the second moment of area of the cross-section of a full beam of depth d and width b is $bd^3/12$, whereas the sum of the second moments of area of two separate beams (but bending together) each of depth (d/2) and width b is $2b(d/2)^3/12 = bd^3/48$, *i.e.* one quarter as much. This assumes an interface of negligible thickness at half-depth of the beam – the effects on flexural stiffness of the interface deviating from half depth (Type 2 variance) and having finite thickness (Type 3 variance)

work counter to each other and will balance out at least to a certain extent. Both k_{full} and k_{non} are reduced by 9% (as shown in the bracket for beams B7-12 and B7-13 in Table 4) when deriving the range of composite action for Group A composite beams to reflect their lower concrete modulus. Data for Group A sprayed concrete beam A7-11 were not used due to the irregular nature of the load-deflection curve, although its flexural stiffness calculates to be 113.6 kN/mm based on 20 GPa Young's modulus, similar to that of beam B7-13.

Table 4 Pre-peak load performance of beams

Type	Beam Ref.	Equivalent flexural stiffness (kN/mm)	Range of degree of composite action
Sprayed concrete beam	B7-12	105.6 (96.1)	
	B7-13	125.4 (114.1)	
Composite beam	A1-11	39.4	0.13-0.21
	A3-11	75.1	0.54-0.71
	A4-11	86.8	0.68-0.87
	B4-12	46.7	0.16-0.26
	B4-13	56.6	0.27-0.38
	A5-11	46.7	0.21-0.31

Post-peak degree of composite action from laboratory load-deflection relationships

In the post-peak load region, the stiffness of both the sprayed concrete and the composite beams degrades with deflection, as shown in Figures 7 and 8, as cracks form and propagate through the beam. Although this region is of less relevance than the pre-peak to the design of SCL in soft ground, as discussed earlier, it could be useful to designers to have confidence that composite mechanical behaviour does not suddenly degrade after peak load and once significant cracking starts.

An analysis was done in which post-peak flexural stiffnesses of the composite beams were compared with that of sprayed concrete beam A7-11 using equation (1) to calculate *DCA*. Detailed presentation of results is beyond the scope of this paper, but *DCA* ranges between 0.52 and 0.88, which is very similar to that obtained from pre-peak strain readings (Table 4). Thus it appears that composite action is indeed maintained post-peak.

Longitudinal strains

Table 5 gives strains measured at 10 kN load for all tested beams. Strains at top and bottom half depth are the average of readings on two sides, whereas strains at top and bottom surfaces are readings from a single strain gauge positioned on the centreline of the cross-section, as shown in Figure 2. Non-zero strain values at half-depth of component beams confirm a certain degree of composite action.

Pre-peak degree of composite action from laboratory longitudinal strains

For Group A beams, longitudinal strain for sprayed concrete beam A7-11 was not available, but its maximum strain at top and bottom half depth (±43.8με) may be calculated from equation (5) assuming 20 GPa Young's modulus. Degree of composite action was then evaluated using equation (2) firstly with the strain at top half depth, then the strain at bottom half depth, giving a range of *DCA* which again should cover variances in beam workmanship as described above.

For Group B beams, top surface (instead of top half) longitudinal strains available for the two sprayed concrete beams were used to calculate using equation (2) the degrees of composite action for each Group B composite beam based on their strains at top half depth. The 12.5% difference in top surface strains for the Group B sprayed concrete beams results in a wider range (compared with using strain at top half) of *DCA* seen in Table 5 that should cover the variations in beam workmanship as described above.

The overall range of degrees of composite action for all composite beams is between 61% and 89%. Data on increase in strain with load for selected beams is shown in Figure 10 confirms the degree of composite action to lie within bounds of 50% and 100%.

Table 5 Longitudinal strain readings at 10 kN load and derived degrees of composite action

Type	Beam Ref.	Strain at top surface	Strain at top half depth	Strain at bottom half depth	Strain at bottom surface	Range of degree of composite action *DCA*
Sprayed concrete beam	B7-12	-70.0	-39.8			
	B7-13	-80.0	-40.2			
Composite beam	A1-11		-33.7	39.7		0.79-0.83
	A2-11		-39.8	36.5		0.84-0.85

A3-11		-43.5	28.1		0.68-0.88
A4-11		-42.5	34.8		0.79-0.89
B4-12	-82.0	-28		109.0	0.68-0.71
B4-13	-73.4	-23.8		92.7	0.61-0.65
A5-11		-35.7	39.8		0.76-0.84

Note: All strains are in microstrain ($\times 10^{-6}$)

Beam end relative displacements

Measured relative displacements for all Group A composite beams were small, less than 0.2 mm, confirming the presence of a high degree of composite action. In summary, all test data showed a certain degree of composite mechanical behaviour existed in the composite beam test specimens.

Numerical simulation of composite mechanical behavior

Routine CSL tunnel design adopts numerical models with design lining thicknesses and specifies tolerances to cover variances in construction. Providing constructed lining thickness is within the tolerance limit, numerical models that use practical values of interface stiffnesses should be able to reflect the impact of this variance on the lining behavior (*i.e.* degree of composite action).

Numerical model for four-point bending

Sprayed concrete in tunnels is usually modelled for design with a linear elastic constitutive model [1], because the large partial factor used in routine design together with variances induced by workmanship during construction far outweigh the potential benefits from a time-consuming nonlinear analysis. Traditional steel reinforcement is then inserted in areas where the linear elastic model predicts from the combination of axial force and bending moment that lining cracks may occur. Pre-peak laboratory data is used to verify the linear elastic numerical results.

The numerical composite beam model, representing the overall dimensions of the idealised beam and its support configuration (Figure 2), is shown in Figure 11. The grid has 288 2D plane strain zones (the standard method for modelling a 2D continuum in FLAC), each 25 mm in length and 18.75 mm in height. Vertical displacement is restrained at the two beam supports. A straight and negligible thickness membrane interface at beam half depth for the composite beams, modelled by interface

elements, is also shown in Figure 11. 5 kN vertical loads are applied at each of the two loading points (10 kN in total). Loading speed is automatically set by the programme according to the stiffness of the structures in the model.

FLAC has a built-in convergence criterion – the maximum unbalanced force ratio, which is a ratio between the algebraic sum and the mean absolute value of forces acting on a FLAC grid-point from its neighbouring elements. A system is usually considered in equilibrium when this ratio is sufficiently small. For this study, it was considered that the system is in equilibrium when the maximum unbalanced force ratio over the grid is less than 10^{-5}.

Model material parameters

The verification approach is to assign appropriate normal interface stiffness K_n and shear interface stiffness K_s ranges as suggested by Su and Bloodworth [8] from element tests in compression, tension and shear, to a numerical model with an idealised geometry. The upper and lower limits of these stiffness ranges will lead to predicted ranges of composite action, which are compared with those observed in the laboratory. If the former covers the latter, it will support the use of the suggested interface stiffness ranges to simulate the behaviour of sprayed concrete linings with their inherent variance.

A linear elastic model was assumed for the interface elements (representing the membrane interface) with tensile and shear strengths of 0.8 MPa and 2.0 MPa respectively, both from the aforementioned laboratory element tests [8].

A linear elastic model was also assumed for the zones (representing sprayed concrete) with a Young's modulus of 20 GPa. Neither compressive nor tensile strength was assigned because the main focus of this numerical analysis was on the pre-peak behavior of composite beams.

Model output

The ranges of K_n and K_s proposed by Su and Bloodworth (2016) and the resulting numerical predicted range of composite action for each composite test specimen are shown in Table 6, which also lists the

laboratory beam deflection and strain derived range of composite action. It can be seen that the predicted ranges of composite action almost all encompass those obtained from tests.

A typical principal stress plot, for the composite beam A-11, is shown in Figure 12. It can be seen that the principal tensile stress (at the bottom of the beam in the horizontal direction) under 10 kN total loading is 1.94 MPa while the principal compressive stress is 2.18 MPa. This difference is mainly due to the stress concentration at the applied loading points and therefore should be ignored. Dividing the principal tensile stress by the Young's modulus of 20 GPa gives a principal tensile strain of around 97×10^{-6}. This is similar to the measured tensile strains under 10 kN total load for composite beams B4-12 (109×10^{-6}) and B4-13 (92.7×10^{-6}) listed in Table 5, and well below the measured cracking flexural tensile strains for composite beam B4-12 (168×10^{-6} under 16.2 kN total load) and B4-13 (237×10^{-6} under 28.5 kN total load).

Table 6 Model predicted and laboratory tested range of composite action

Beam Ref.	K_n input range (GPa/m)	K_s input range (GPa/m)	Predicted range of composite action *DCA*	Laboratory beam deflection derived range of composite action *DCA*	Laboratory beam strain derived range of composite action *DCA*
A1-11	10-16	0.3-6.7	0.29-0.81	0.13-0.21	0.79-0.83
A2-11	10-16	0.3-6.7	0.29-0.81		0.84-0.85
A3-11	4.0-10	0.9-9.3	0.40-0.84	0.54-0.71	0.68-0.88
A4-11	1.0-4.0	0.3-3.0	0.26-0.64	0.68-0.87	0.79-0.89
A5-11	1.0-4.0	0.3-3.0	0.26-0.64	0.21-0.31	0.76-0.84
B4-12	1.0-4.0	0.3-3.0	0.26-0.64	0.16-0.26	0.68-0.71
B4-13	1.0-4.0	0.3-3.0	0.26-0.64	0.27-0.38	0.61-0.65

Averaging *DCA* from strains and deflections gives a new best estimate of composite action ratio range from tests, listed in the 4th column in Table 7. A set of 'best-fit' interface stiffnesses (5th column of Table 7) may then obtained from the model by trial from within the initially suggested ranges, to match as closely as possible these average laboratory ratios (4th column of Table 7).

Best-fit K_n values show a clear trend of being close to or even beyond the upper limits of the suggested ranges from element tests when membrane thickness increases. The deformation mode in the element

tests used to obtain K_n was observed to involve transverse tension with visible squeezing out of the membrane in the case of thicker membrane samples (2016). The membrane is much more constrained in the beam test against this kind of effect, which is the likely explanation for the apparent higher K_n seen in the beam tests.

For K_s the situation is less clear-cut. Best-fit values lie within the suggested range from element tests, mostly around the average value but lower in the case of the smooth thin membrane interface (A1-11) or higher in the case of the smooth thick membrane interface (A4-11). It is difficult to draw definite conclusions from the small dataset, but it appears that the shear element tests used to obtain K_s are reasonably representative of the beam situation.

It should be noted that this set of best-fit interface stiffnesses is not intended for use in design, but as a starting point for the interface stiffness sensitivity study described in the next section.

Table 7 Model predicted range of composite action and best-fit interface stiffnesses from beam test data

Beam Ref.	K_n input range (GPa/m)	K_s input range (GPa/m)	Average laboratory derived composite action	Best-fit K_n/K_s (GPa/m)
A1-11	10-16	0.3-6.7	0.49	12/1.1
A2-11	10-16	0.3-6.7	0.84*#	10/9.3
A3-11	4.0-10	0.9-9.3	0.71	8.0/4.0
A4-11	1.0-4.0	0.3-3.0	0.81#	16/6.7
A5-11	1.0-4.0	0.3-3.0	0.53	4.0/1.7
B4-12	1.0-4.0	0.3-3.0	0.45	4.0/1.2
B4-13	1.0-4.0	0.3-3.0	0.48	4.0/1.4

* Only strain data available # out of the predicted range of composite action

Sensitivity studies on the degree of composite action

The beam numerical model was used to examine the impact of variation of interface stiffness (caused for example by using a different type of membrane or the same membrane under different conditions of temperature or humidity) and of membrane interface position on the degree of composite action, R_c. In the first sensitivity study, normal interface stiffness K_n and shear interface stiffness K_s, were varied both individually and simultaneously by a factor of 10 either side of base values K_n=8 GPa/m and

K_s=4 GPa/m selected from beam A3-11 (for which *DCA* = 0.71). Sprayed concrete Young's modulus was taken as 20 GPa.

Sensitivity studies model output

Results from varying K_n and K_s independently are shown in Figure 13, in which the interface stiffnesses on the horizontal axis are normalised to their base values. *DCA* is more sensitive to K_s than to K_n, although reductions in K_n have more effect than increases.

Sensitivity of *DCA* to K_n and K_s varying simultaneously is illustrated in the contour plot Figure 14 and the detailed results are given in Appendix B. Over the range of K_n and K_s as a whole, there is significant change in *DCA*, varying from 0.07 to 0.96 over 0.1 to 10 times base case K_n and K_s values. Over the range 0.2 to 2 times base case K_n and K_s, *DCA* varies between 0.30 and 0.83, which reflects the spread of composite action ratios calculated from the laboratory data (and listed in Tables 4 and 5).

Impact of membrane interface position on composite action ratio was also investigated by means of a sensitivity study. Interface position was varied from near the bottom surface of the beam to near the top, whilst maintaining constant overall beam depth of 150 mm.

Figure 15 shows the beam deflections and composite action ratios thus obtained as a function of the ratio of top component beam thickness to overall beam depth. Both composite action ratio and beam deflection are greatest when the membrane is at mid-depth. Although increasing one component beam thickness (and reducing the other) reduces beam deflection by increasing the overall moment of inertia, the composite action ratio is actually reducing as the membrane position moves towards the extreme fibres. When the membrane interface is at the mid-depth, the difference in deflection between non-composite and composite beams is greatest, demonstrating the composite action is maximum. This follows elastic beam theory in which longitudinal shear stress is maximum at mid-depth of a beam under bending. An interface placed at this location will experience the greatest possible shear stress mobilised on it, leading to the highest composite action ratio. Figure 16 also shows that the membrane interface deviation less than 10% (ratio between 0.45 and 0.55) from the half-depth of overall beam has little impact on the degree of composite action.

Discussion of results

Condition of laboratory specimens with respect to tunnel conditions

CSL tunnels using spray-applied membrane in soft ground are still a very recent and innovative lining configuration. Until now there is no in-situ testing data available regarding the actual membrane humidity condition in the CSL configuration in the long term. The samples used in this study were stored under ambient laboratory conditions, which is likely to be drier than the in-situ condition. On the one hand, the main purpose of this research is to develop and validate a numerical modelling approach for simulating the composite mechanical behaviour, and it is better to avoid introducing membrane saturation as an additional variable in the calibration, as its impact can be directly reflected by varying the spray-applied membrane interface properties in the numerical model once calibrated. On the other hand, the laboratory measured values of strength and stiffness are likely to be high compared to the in-situ values and therefore should not (along with the derived variable of degree of composite action) be used directly for design but rather as indicative and for calibration of the numerical model. Further investigations of realistic humidity conditions in CSL structures, and their influence on membrane properties, is required to provide realistic membrane interface input data for the full CSL tunnel design.

Implications of small scale test and short-term loading

Again because CSL tunnels are a recent innovation that has only been used for a few projects, so far there are no long-term in-situ testing data available. In this research, composite beams were laboratory tested only under short-term loading, which does not precisely reflect the real long-term behavior of CSL tunnels. However, plentiful research literature has been published on the ground response and lining behavior of SCL tunnels in both short and long terms. With the gradual understanding of the spray-applied membrane interface mechanical properties in both short and long terms, the behavior of CSL tunnels should be predicted fairly accurately using numerical modelling, which is a topic of the next stage of research.

Impact of variances in sample workmanship on the measured values

In this research, flexural response of all tested beams is presented and their general behaviour commented on. The ranges of *DCA* obtained for each composite beam from beam deflection and longitudinal strain data are quite tight (mostly around 10%) and generally lower from the former than from the latter. These differences are attributed mostly to the three types of variances in sample workmanship noted previously and their impact on the external (deflection) and local (strain) measurements. Strains should inherently be more accurate because they are local measurements. However, they have the disadvantage of being only 'point' measurements, which brings its own variance issues. Therefore, an averaged value of laboratory beam deflection and strain derived composite action ratio is used to derive the best-fit interface stiffness in this study. Detailed analysis of the effect of this assumption is beyond the scope of this paper.

Comparison of beam deflection from numerical modelling and laboratory tests

Beam midspan deflections predicted by the FLAC model using the best-fit and the upper and lower limit interface stiffnesses listed in Table 7 were compared with laboratory measurements, as shown in Figure 16 for Types 4 and 5 composite beams. Types 1, 2 and 3 beams are not included in the comparison mainly because of their midspan deflection errors caused by the three variances. Comparison was only carried out between 0 and 10 kN total load to avoid any nonlinearity at higher load level.

It can be seen that the numerically predicted midspan deflections using the laboratory test obtained upper and lower limit interface stiffnesses are able to cover three of the four laboratory measured beam midspan deflections. The larger deflection of beam 4-12 at the initial stage compared to the numerically predicted deflection curve using the lower limit interface stiffness is due to a "bedding effect" (where the beam exhibits lower stiffness during initial loading as it settles on its supports), after which the deflection curve gradually moves closer to the numerically predicted values. The laboratory tested deflection curve of beam A4-11 also shows a strong "bedding effect" at the initial stage but later on moves closer to the numerical predicted deflection curve using the upper limit

interface stiffness. The laboratory test deflection curves of the other two beams (A5-11 and B4-13) are very close to the numerical predicted deflection curve using the best fit interface stiffness.

This comparison shows that the beam numerical model using the laboratory test obtained interface stiffnesses generates inclusive results. The use of additional potentiometers improves the reliability of the external measured beam deflection values. Further investigation on the comparison of longitudinal strains from numerical modelling and laboratory tests is presented in the following section.

Comparison of beam longitudinal strains from numerical modelling and laboratory tests

Longitudinal strains predicted by the FLAC model using the best-fit and the upper limit interface stiffnesses listed in Table 7 were compared with laboratory measurements, as shown in Figure 17 for two selected Group B composite beams. Considering their best-fit interface stiffnesses are very close, only one line representing the best-fit FLAC prediction is shown. Strains predicted by the numerical model show a reversing strain profile, as shown in Figure 17, giving clear evidence of shear transfer through the membrane interface. This reversing strain profile is also observed in the strain measurement profiles found by Nakashima *et al*. [7]. Figure 17 shows the longitudinal strains predicted by FLAC model using the upper limit interface stiffnesses are very close to the laboratory tested results, whereas those using the best-fit interface stiffnesses over-predict the strains. From designers' point of view, the beam numerical model using both interface stiffnesses generates conservative results, giving confidence to the lining safety of CSL tunnels. It also shows that at least two strain gauges positioned at different depths on each component are necessary to accurately identify the reversing nature of strain distribution from laboratory tests.

Comparison of beam end relative displacements from numerical modelling and laboratory tests

The numerical predicted beam end relative displacements between the top and bottom components for all beams under 10 kN total load using laboratory test obtained interface stiffnesses are between 0.006 mm and 0.021 mm respectively, much smaller than the laboratory test obtained value around 0.2mm. This is likely to be because linear potentiometers are unable to accurately detect the displacement at that magnitude.

Conclusions

A series of laboratory tests have been carried out on fibre-reinforced sprayed concrete beams with sandwiched spray-applied waterproofing layer, representing elements of a CSL tunnel lining, followed by a series of numerical analyses to calibrate a numerical approach for simulating the composite mechanical action of the CSL beams. The following conclusions can be drawn from this research:

- The tests under ambient laboratory climate conditions showed clear evidence of a certain degree of (although not full) composite mechanical behaviour, from measured deflections and strains and very small relative beam end displacements. Beams failed by growth of a single crack at midspan, and showed significant plateaus of residual stress after peak load.
- Test results were used to verify a numerical model of a composite beam assuming an interface of negligible thickness at half-depth of the beam using interface elements for the membrane interface, stiffness properties of which could be adjusted to simulate a range of factors, such as primary substrate roughness, membrane thickness and membrane humidity conditions.
- Degree of composite action ratios predicted by the model were in reasonable agreement with the test data (which was all for 'dry' samples) taking into account variance in test specimen geometries due to workmanship, and test procedures.
- Back analysis indicates that the apparent normal stiffness K_n in the beam tests was generally higher than that measured in compressive element tests, which fits with observation of transverse deformation of the membrane in those tests, whereas K_s was generally around the average measured values, demonstrating reasonably good quality data from shear element tests.
- The model was then used for sensitivity studies to investigate the effect on degree of composite mechanical behaviour of variation in interface stiffness and primary/secondary lining thickness ratio (or membrane position). Variation in degree of composite action (DCA) from varying interface stiffness (generally caused by constructional issues such as variation in substrate surface preparation, and membrane thickness) was found to be from approximately 30% - 80%, compared to a base DCA of 71%. A smaller range is observed from varying membrane position.
- The sensitivity studies show increasing *Kn* and/or *Ks* will increase the degree of composite action, with *Ks* having greater effect. Composite mechanical behaviour is greatest when the

membrane is at half-depth of the lining.

Designers or contractors involved in future projects may procure their own element tests to obtain interface stiffness parameters appropriate to their lining design and then utilise the output of the numerical sensitivity study described in this paper to estimate the degree of composite mechanical behaviour to design their lining. In the next stage of research, numerical modelling procedures established herein will be applied to a whole tunnel in a fully coupled model including ground and groundwater. Sensitivity of whole tunnel lining performance to membrane interface parameters and robustness (in particular that of the interface) under external loadings will be investigated and optimisation of overall lining thickness to reflect the existence of composite mechanical behaviour will be attempted.

Acknowledgements

The authors gratefully acknowledge the financial support of Mott MacDonald and Normet in carrying out this study. Experimental work was carried out in the laboratories of the Faculty of Engineering and the Environment at the University of Southampton.

Appendix A Test specimen materials

Type	Source
Spray-applied membrane	TamSeal 800
CEM1	Cemex- Rugby
0/4 MP Sand	Cemex - Northfleet
4/10 Gravel	Cemex - Northfleet
Water reducing admixture	Cemex – CP105 (ml)
Steel fibre	Dramix
Superplasticiser	TamCem 60
Accelerator	TamShot 800

Appendix B Degree of composite action with varying K_n and K_s simultaneously

	K_s (GPa/m)

		0.1	0.2	0.5	1	2	5	10
	10	0.34	0.43	0.60	0.74	0.84	0.93	0.96
	5	0.34	0.43	0.60	0.73	0.84	0.92	0.96
	2	0.33	0.42	0.60	0.73	0.83	0.92	0.95
K_n (GPa/m)	1	0.32	0.41	0.58	0.71	0.82	0.90	0.94
	0.5	0.29	0.39	0.56	0.69	0.79	0.88	0.91
	0.2	0.21	0.30	0.47	0.61	0.71	0.80	0.83
	0.1	0.07	0.17	0.34	0.47	0.57	0.66	0.69

References

ACI. 2008. ACI318: Building Code Requirements for Structural Concrete (ACI318-08) and Commentary (ACI318R-08). American Concrete Institute: Farmington Hills.

Batty, E., Kentish, E., Skarda, A., 2016. Robotic Application of a 50mm Thick Sprayed Concrete Fireproofing Layer. In: Proceedings of World Tunnel Congress 2016. Red Hook: Curran Associates Inc. pp 733-42.

Bergado, D.T., Teerawattanasuk, C., 2008. 2D and 3D numerical simulations of reinforced embankments on soft ground. Geotextiles and Geomembranes, 26(1), pp 39-55.

Bloodworth, A., Zhou, X., 2014. Acoustic Emission Testing of Fibre Reinforced Concrete Tunnel Lining Samples. In: Proceedings of 7th International Symposium on sprayed concrete. Oslo: Tekna. pp 98-111.

BSI. 2006. BS EN 14488-3: Testing Sprayed Concrete – Part 3: Flexural strengths (first peak, ultimate and residual) of fibre reinforced beam specimens. London: British Standards Institute.

BSI. 2005. BS EN 14651: Test methods for metallic fibre concrete. Measuring the flexural tensile strength (limit of proportionality (LOP), residual). London: British Standards Institute.

BSI. 2005. BS-EN 14487-1: Sprayed Concrete – Part 1: Definitions, specifications and conformity. British Standards Institute.

CIA, 2011. Shotcreting in Australia: Recommended Practice, 2nd ed. Concrete Institute of Australia & AuSS, Sydney.

Chen, C.Y., Martin, G.R., 2002. Soil–structure interaction for landslide stabilizing piles. Computers and Geotechnics, 29(5), pp 363-86.

fib, Bulletin No. 65: Model Code 2010 - Final draft, 2013. The International Federation for Structural Concrete. Berlin: Ernst & Sohn.

Frankl, B.A., Lucier, G.W., Hassan, T.K. and Rizkalla, S.H., 2011. Behavior of precast, prestressed concrete sandwich wall panels reinforced with CFRP shear grid. PCI journal, 56(2), pp 42-54.

Green, R.A., Ebeling, R.M., 2003. Modeling the dynamic response of cantilever earth-retaining walls using FLAC. In 3rd International Symposium on FLAC: Numerical Modeling in Geomechanics, Sudbury, Canada.

Hasik, O., Junek, J., Zamecnik, M., 2015. Metro Prague – use of sprayed waterproofing membrane in deep level station. In: Davorin, K., (Ed.), Proceedings of the ITA World Tunnel Congress 2015, Zagreb, HUBITG.

Holter, K.G., 2016. Performance of EVA-Based Membranes for SCL in Hard Rock. Rock Mechanics and Rock Engineering, Volume 49, Issue 4, pp 1329-1358. DOI 10.1007/s00603-015-0844-5

Holter, K.G., Bridge, R., Tappy, O., 2010. Design and construction of permanent waterproof tunnel linings based on sprayed concrete and spray-applied double-bonded membrane. In: Jaromír, Z., (Ed.), Proceedings of the 11th international conference underground constructions Prague, Czech Tunnelling Ass. ITA-AITES, pp. 121-26.

Holter, K.G., Geving, S., 2015. Moisture transport through sprayed concrete tunnel linings. Rock Mech Rock Eng. DOI 10.1007/s00603-015-0730-1

Itasca, 2008. FLAC version 6.0 Fast Lagrangian Analysis of Continua, Theory and Background, User Manual. Minneapolis: Itasca Consulting Group Inc.

ITA. 2013. ITAtech Report No. 2. Design Guidance for Spray Applied Waterproofing Membranes. International Tunnelling Association. Available at http://www.ita-aites.org/en/future-events/644-design-guidance-for-spray-applied-waterproofing-membranes

Jones, B., 2007. Stresses in sprayed concrete tunnel junctions. Doctoral dissertation, University of Southampton.

Jones, B., Thomas, A., Hsu, YS., Hilar, M., 2008. Evaluation of innovative sprayed-concrete-lined tunnelling. Proceedings of the ICE-Geotechnical Engineering, 161(3), pp 137-49.

Nakashima, M., Hammer, A.L., Thewes, M., Elshafie, M. and Soga, K., 2015. Mechanical behaviour of a sprayed concrete lining isolated by a sprayed waterproofing membrane. Tunnelling and Underground Space Technology, 47, pp.143-152. http://dx.doi.org/10.1016/j.tust.2015.01.004.

NCA, 2011. Norwegian code of practice; Publication No 7, Sprayed Concrete for Rock Support – Technical Specification, Guidelines and Test Methods; Norwegian Concrete Association, Oslo.

Pickett, A., 2013. Crossrail sprayed concrete linings design. In: Anagostou, G., Ehrbar, H., (Eds.), Underground. The Way to the Future. Abingdon: CRC Press, pp. 956-63.

Pickett, A.P. and Thomas, A.H., 2011. The design of composite shell linings. In Proceedings of Sixth International Symposium on Sprayed Concrete, Tromso, Norway pp. 402-413.

RILEM TC 162-TDF, 2003. Test and design methods for steel fibre reinforced concrete. σ-ε-design method, final recommendation. Materials and Structures, 36(8): pp 560-67.

Su, J., 2013. Design of sprayed concrete lining in soft ground – a UK perspective. In: Anagostou, G., Ehrbar, H., (Eds.), Underground. The Way to the Future. Abingdon: CRC Press, pp. 593-600.

Su, J. and Bloodworth, A., 2016. Interface parameters of composite sprayed concrete linings in soft ground with spray-applied waterproofing. Tunnelling and Underground Space Technology, 59, pp.170-182.

Thomas, A., 2003. Numerical modelling of sprayed concrete lined (SCL) tunnels. Doctoral dissertation, University of Southampton.

Thomas, A., 2010. Advances in sprayed concrete tunnelling. Tunnelling Journal 2010, April/May, pp. 40-44.

Verani, C.A., Aldrian, W., 2010. Composite linings: ground support and waterproofing through the use of a fully bonded membrane. In: Bernard, E.S., (Eds.), Shotcrete: Element of a System. Taylor & Francis, London, pp. 269-282.

Figures

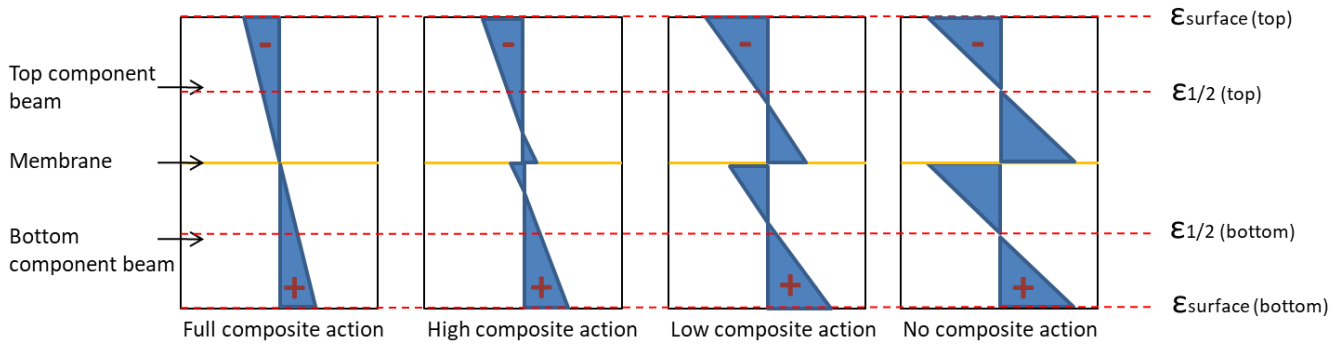

Figure 1 Stress and strain distributions through linings for different degrees of composite action assuming linear elastic behavior

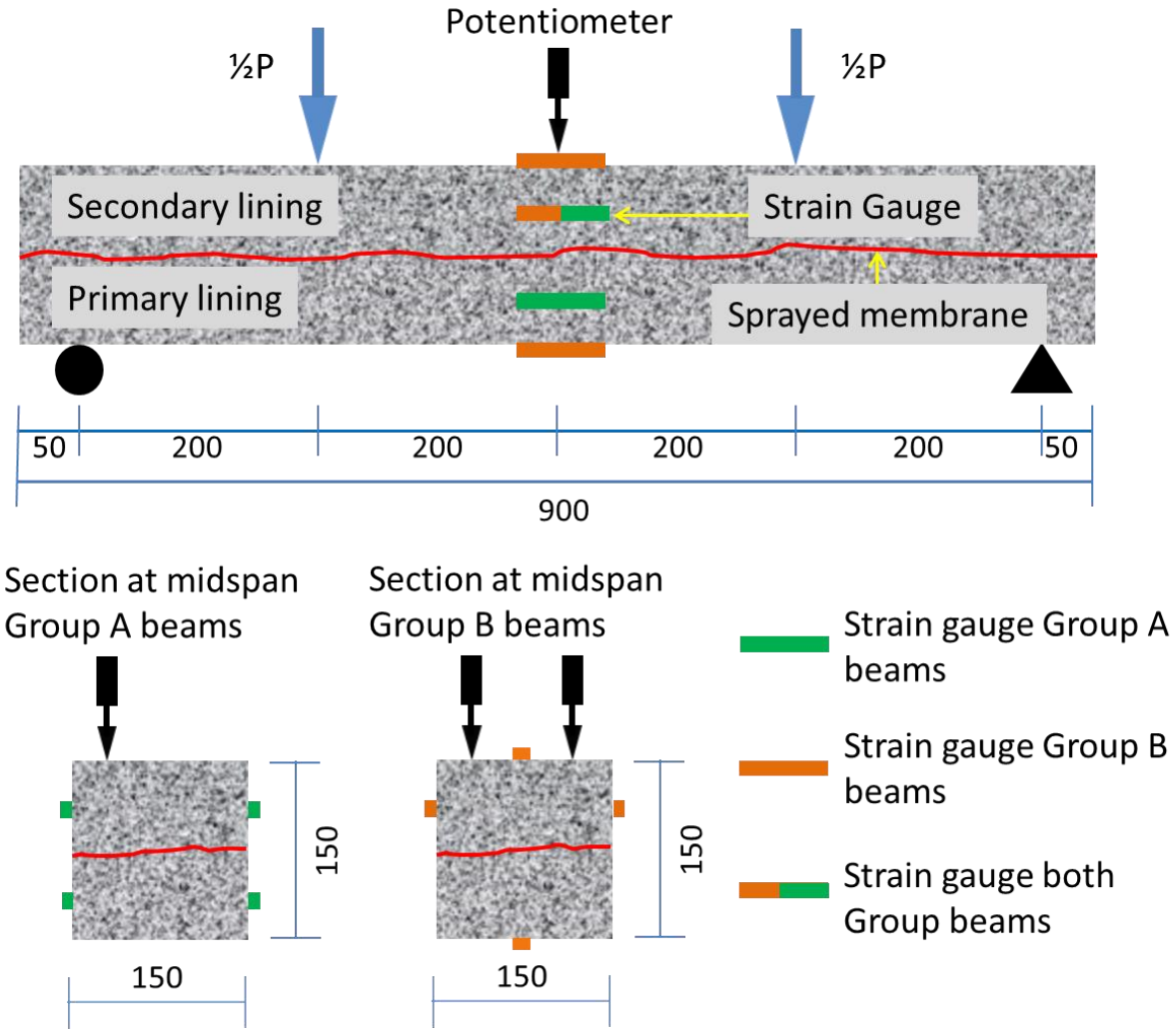

Figure 2 Configuration of four-point bending test on composite beam (all dimensions are in mm)

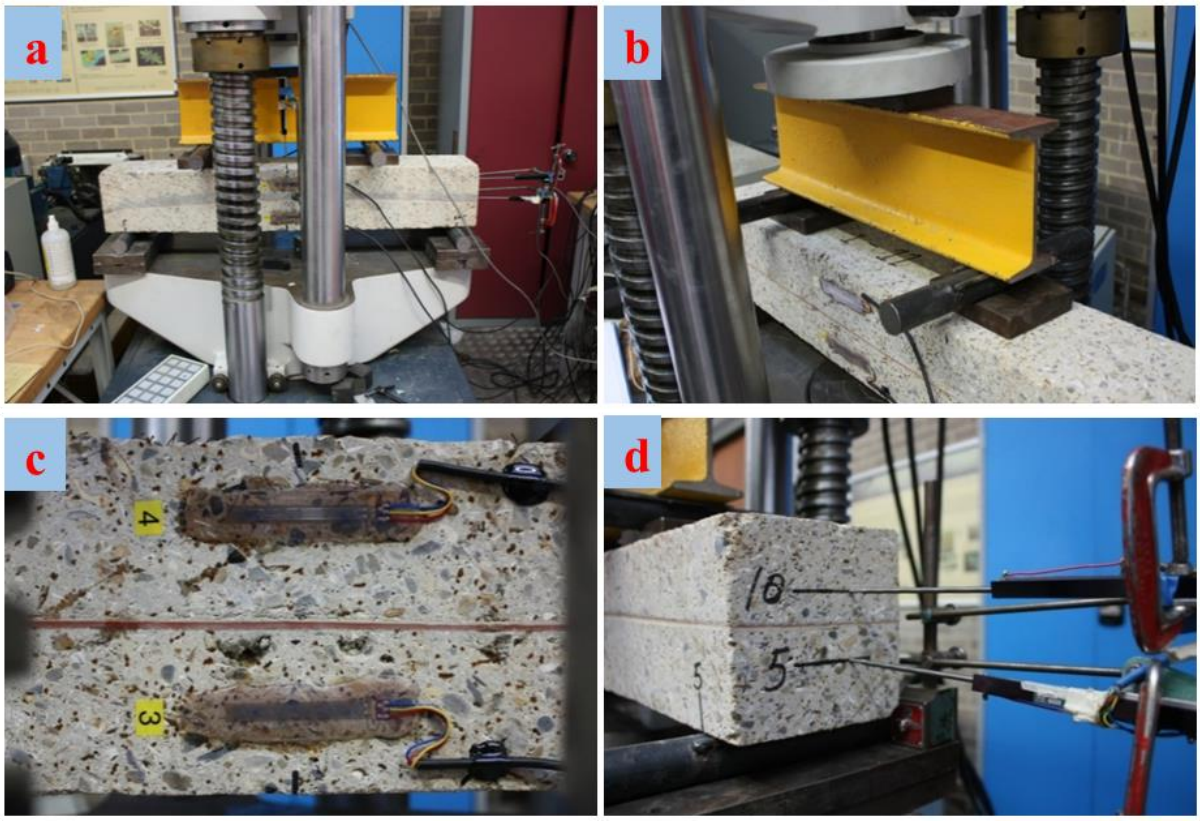

Figure 3 (a) Group A four-point bending test with one potentiometer (b) load transfer configuration (c) strain gauges measuring longitudinal strain (d) potentiometers measuring beam end displacements

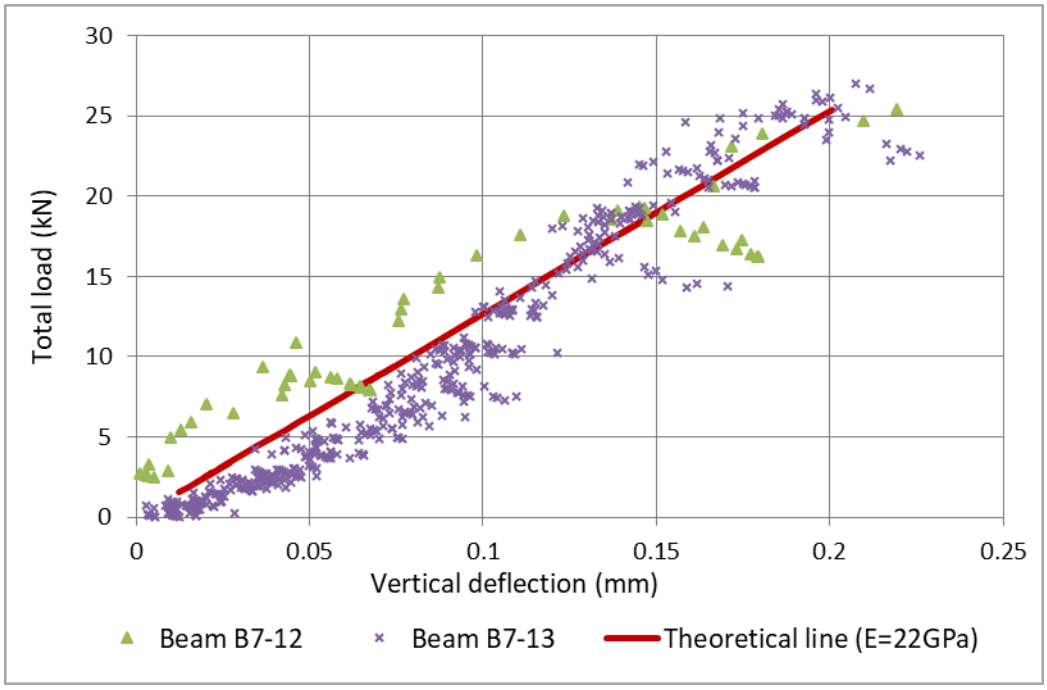

Figure 4 Concrete Young's modulus obtained from load-deflection relationships for Group B sprayed concrete beams

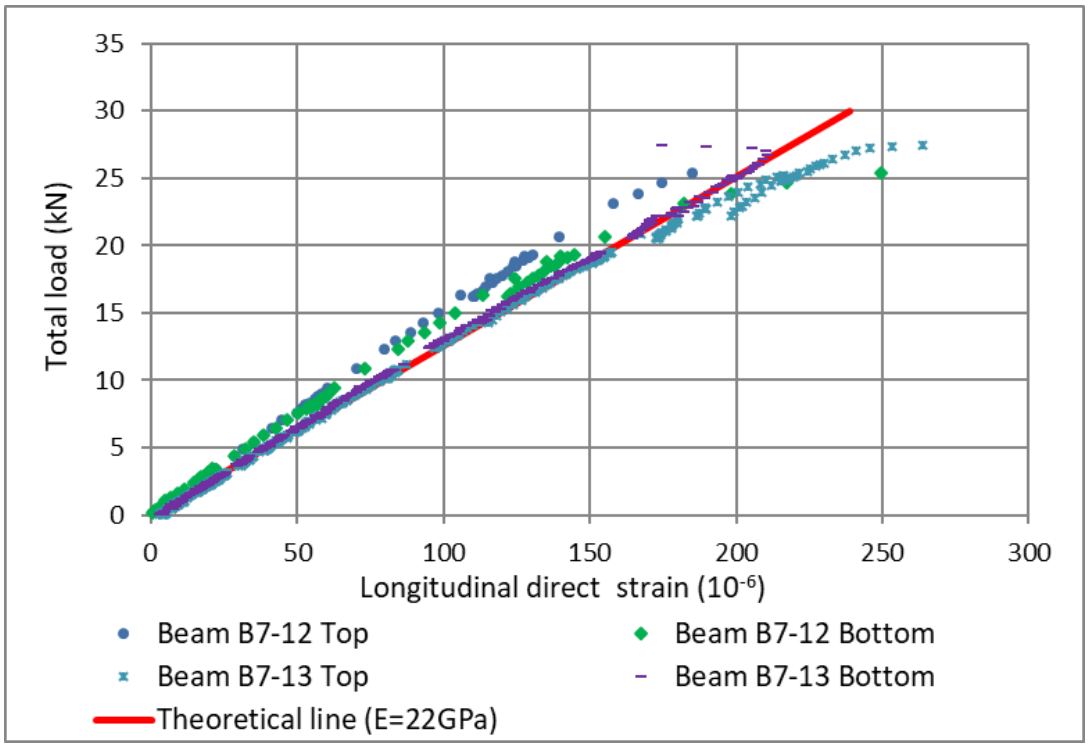

Figure 5 Concrete Young's modulus obtained from pre-peak load longitudinal strains for Group B sprayed concrete beams

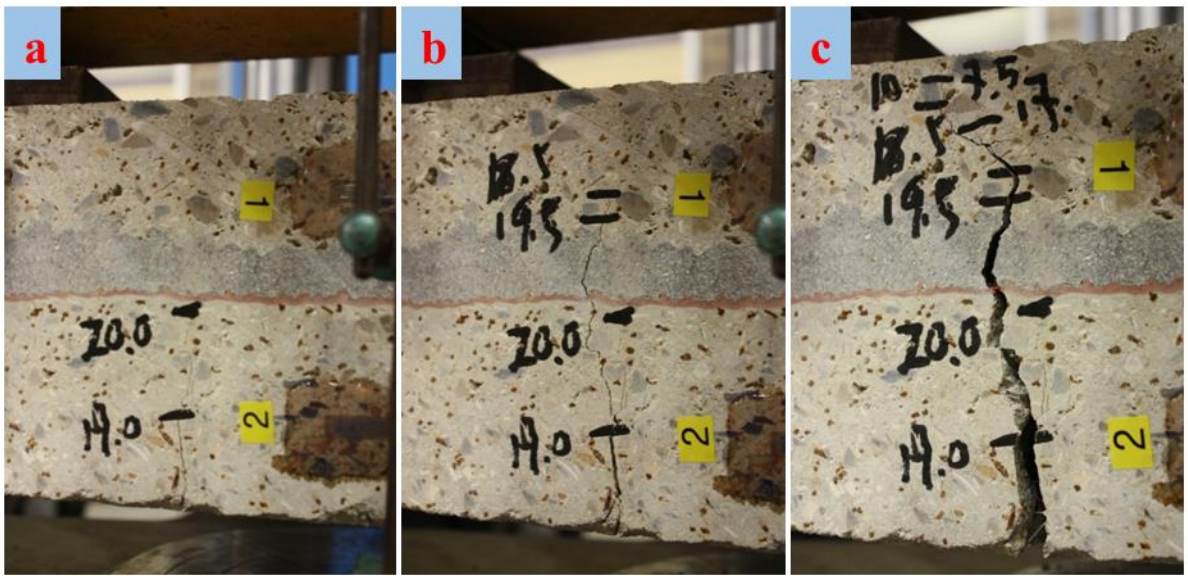

Figure 6 Crack development during the test for beam A2-11(a) approaching peak load (b) passing peak load (c) residual strength

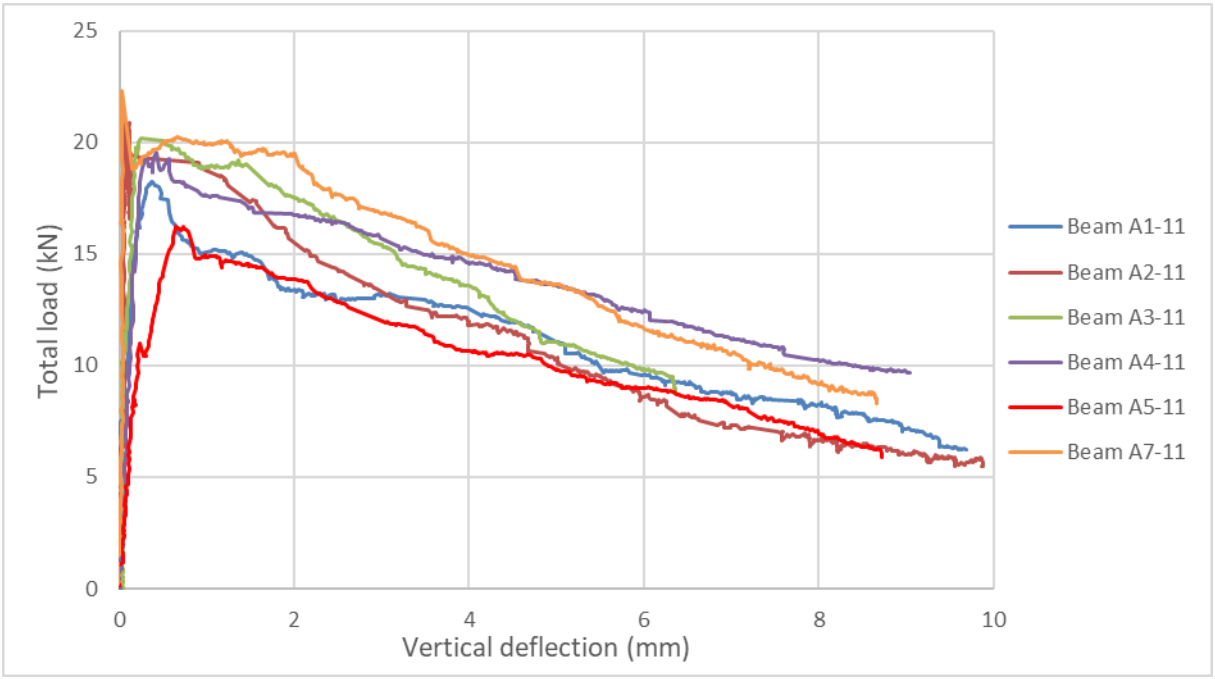

Figure 7 Load-deflection relationships for Group A beams

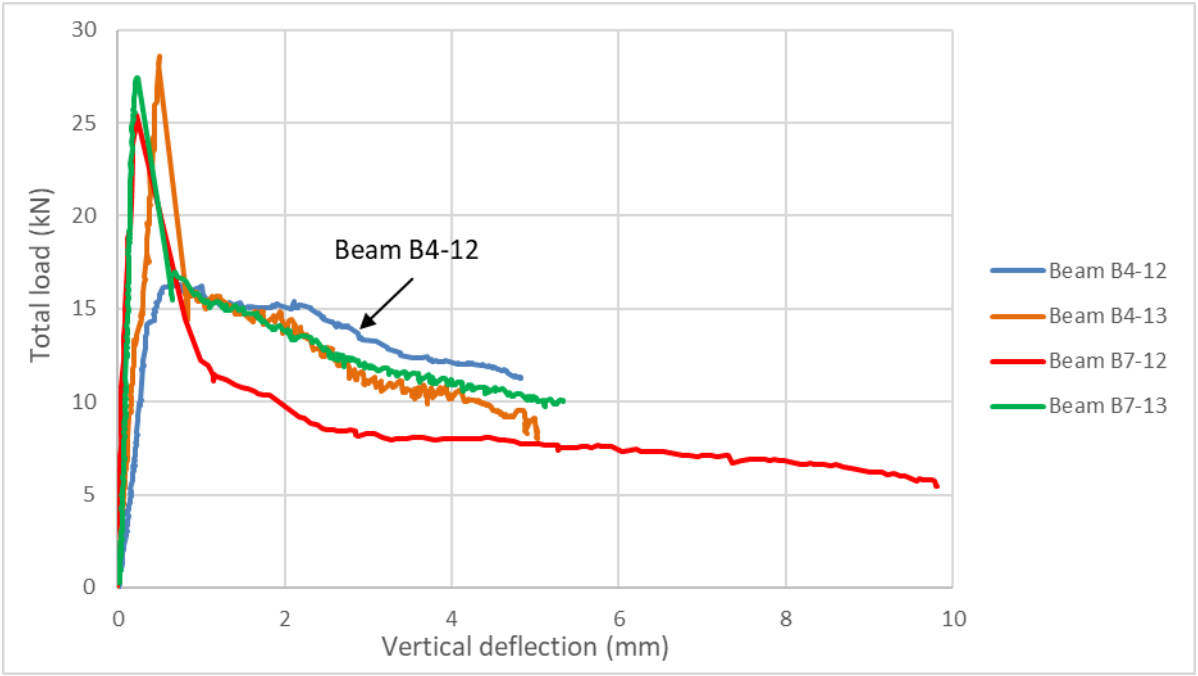

Figure 8 Load-deflection relationships for Group B beams

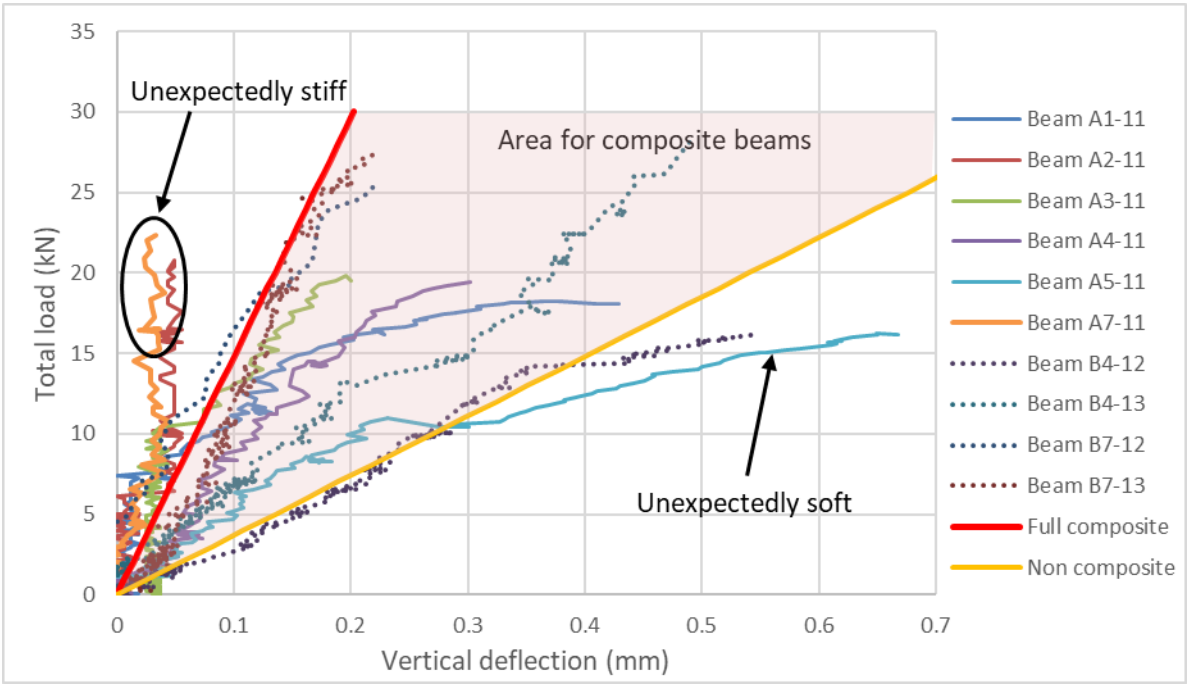

Figure 9 Pre-peak load load-deflection relationships for all test beams

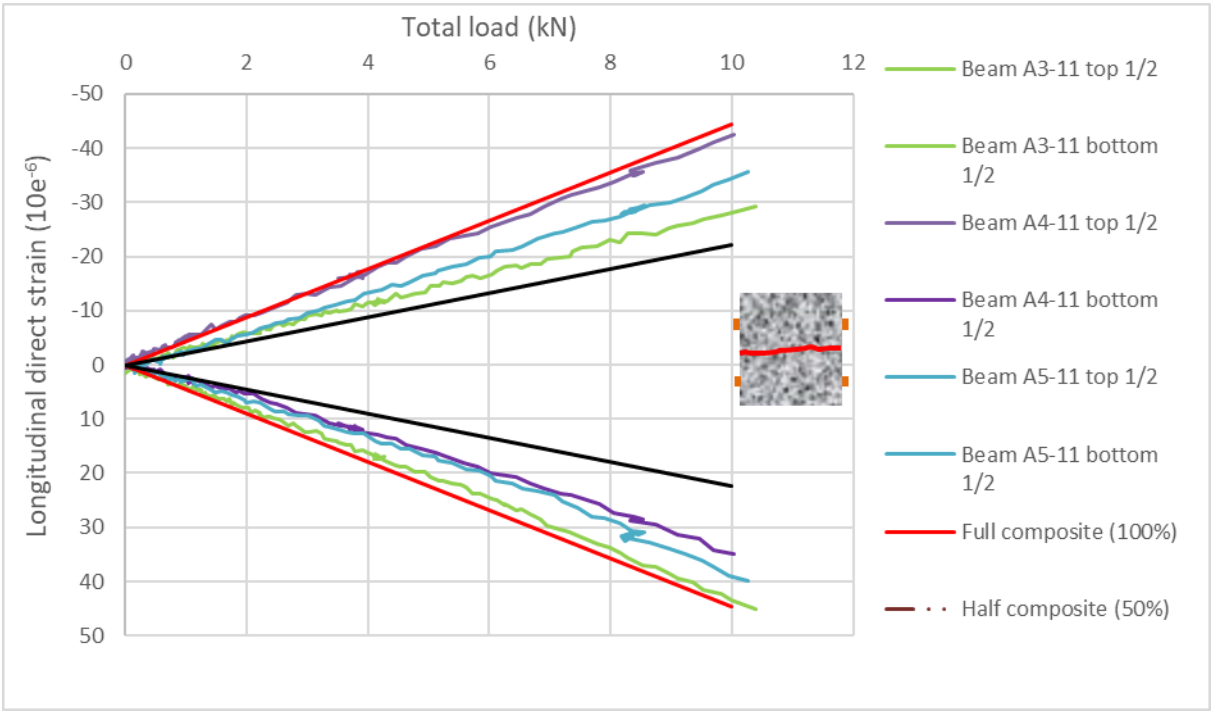

Figure 10 Pre-peak load longitudinal strains for selected composite beams

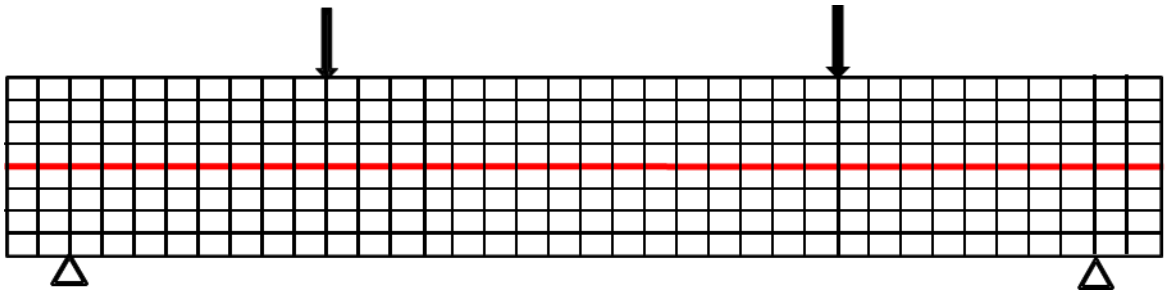

Figure 11 Geometry, loading and boundary conditions for a composite sprayed concrete beam FLAC model

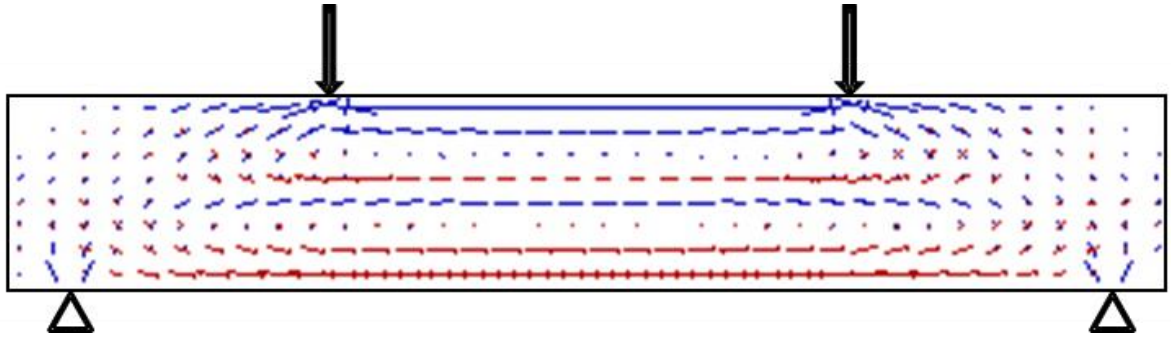

Figure 12 Principal stress for a composite sprayed concrete beam predicted by a FLAC model

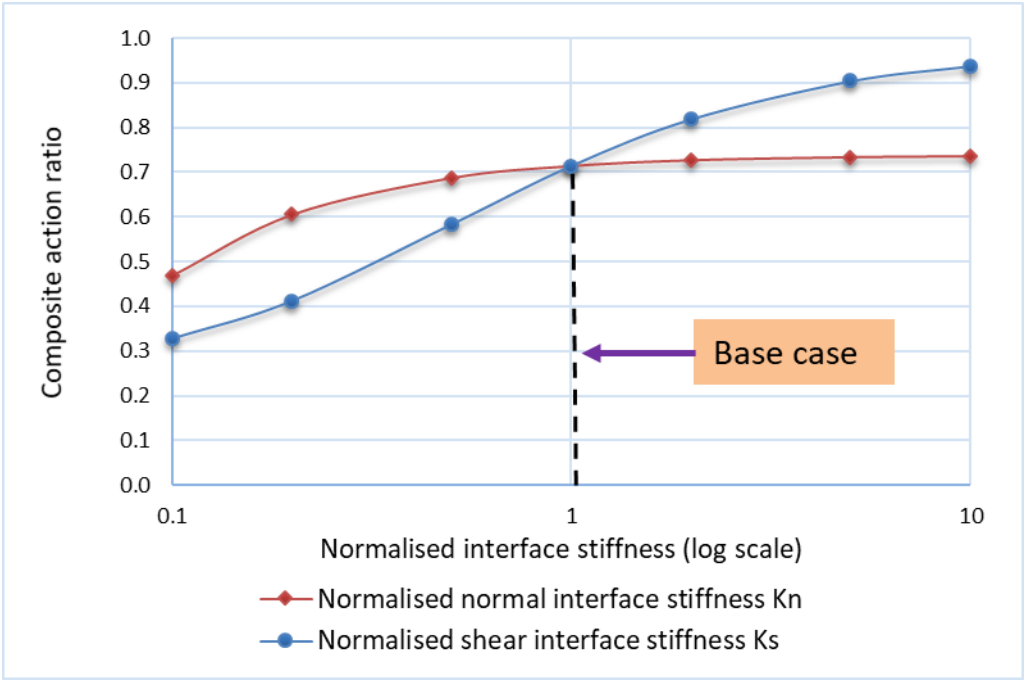

Figure 13 Sensitivity of composite action ratio to normalised K_n and K_s varying independently

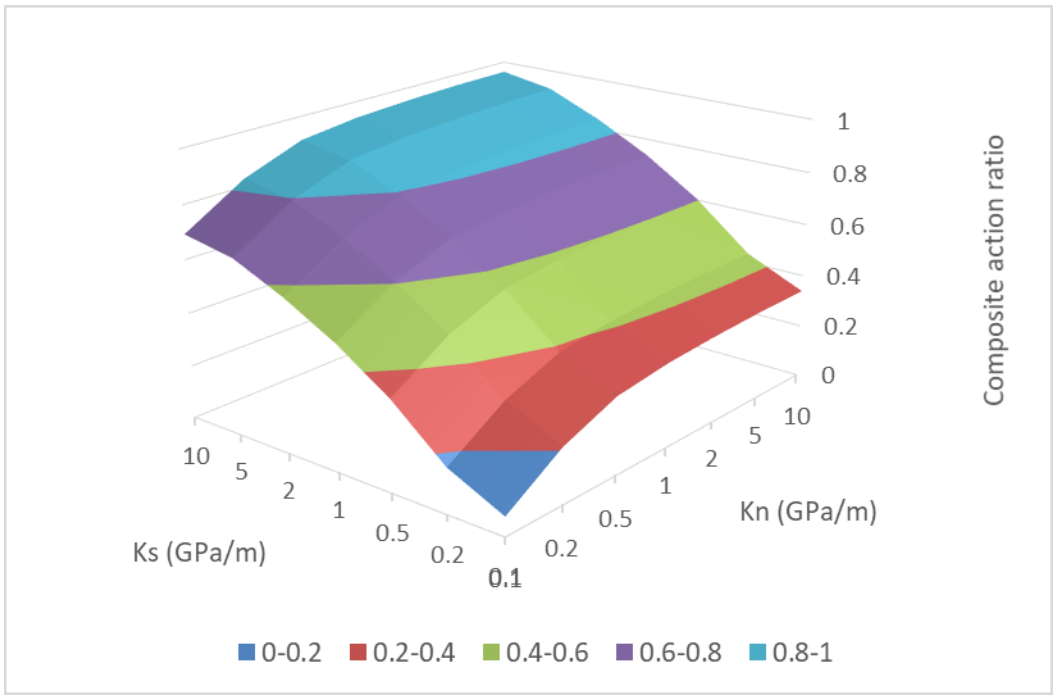

Figure 14 Sensitivity of composite action ratio to normalised K_n and K_s varying simultaneously

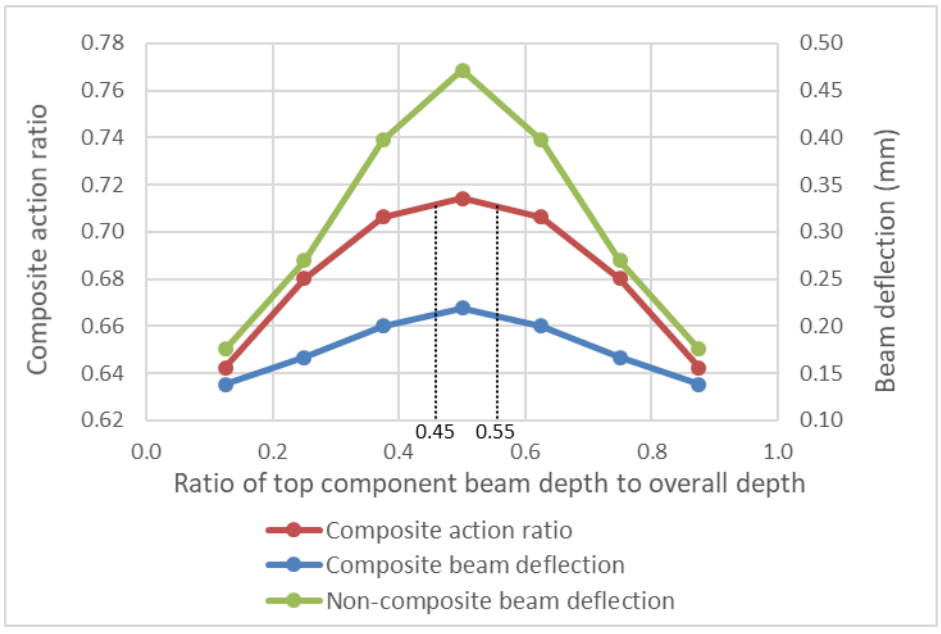

Figure 15 Beam deflection and composite action ratio as a function of membrane interface position

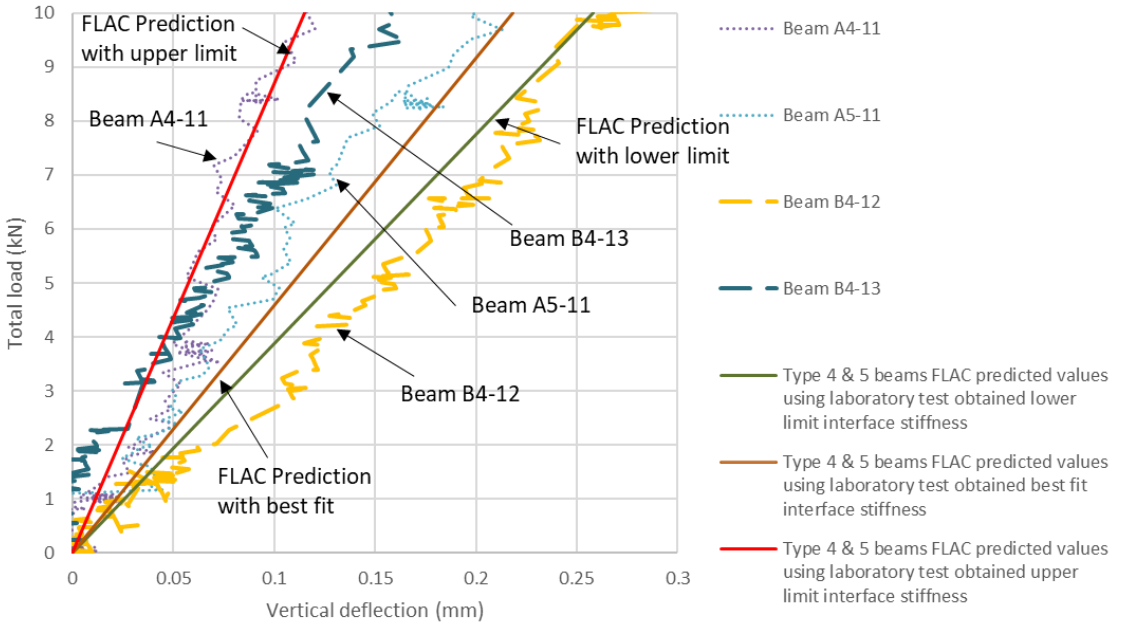

Figure 16 Vertical displacement predicted by FLAC model and obtained from laboratory tests for typical composite beams

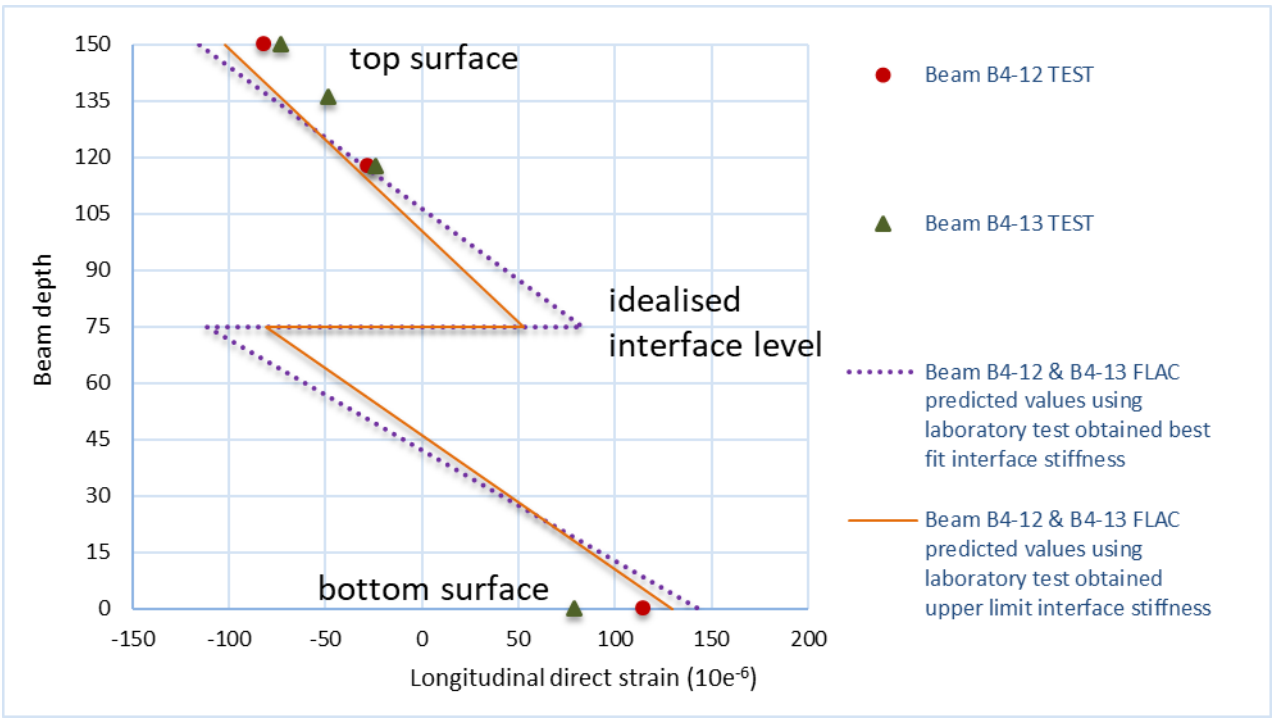

Figure 17 Longitudinal strains predicted by FLAC model and obtained from laboratory tests for typical composite beams